# An effective method based on time reversal and optimization techniques for locating faults on power grids

Moussa Kafal, Nicolas Gregis, Jaume Benoit, Nicolas Ravot

## HAL Id: cea-03122180
## https://cea.hal.science/cea-03122180

# An Effective Method Based on Time Reversal and Optimization Techniques for Locating Faults on Power Grids

**4 authors**, including:

Moussa Kafal
Atomic Energy and Alternative Energies Commission
**40** PUBLICATIONS   **191** CITATIONS

Nicolas Ravot
Atomic Energy and Alternative Energies Commission
**28** PUBLICATIONS   **207** CITATIONS

Some of the authors of this publication are also working on these related projects:

Advances in reflectometry techniques for complex transmission line network diagnosis View project

FLOW-CAM View project

# An Effective Method Based on Time Reversal and Optimization Techniques for Locating Faults on Power Grids

Moussa Kafal, *Member, IEEE*, Nicolas Gregis, Jaume Benoit and Nicolas Ravot

*Abstract*—**Electromagnetic time reversal (EMTR) has recently emerged as a promising technique applied for locating faults in power networks. It directly transposes the idea of focusing energy back to its source introduced in original time-reversal (TR) methods. Accordingly, we present in this paper, FasTR, a method based on the tenets of TR, that estimates the fault location by employing optimization based algorithms for fetching the highest peak amplitude with maximum coherence in *space* and *time*. However, it uses an alternative approach for executing the cumbersome TR post-processing, thanks to a simplified analytical model capable of evaluating the voltage (or current) at any position and any instant of the tested network resulting from the back-injection of the recorded time-revered signals. FasTR is shown to accurately locate a fault in a complex network with just a basic knowledge of its topology in no more than a couple tens of seconds. More importantly is its ability to locate multiple faults in non-homogeneous networks. The performance of the proposed method is validated by numerical simulations as well as an experimental setup by making reference to a reduced-scale coaxial cable network where real faults are hardware-emulated.**

*Index Terms*—**Electromagnetic time reversal, fault location, optimization techniques, power system faults, power system transients, power system protection.**

## I. INTRODUCTION

**G**LOBAL demand for electrical energy is increasing rapidly, because of population and economic growth, especially in emerging economies. While accompanied by greater prosperity, rising demand creates new challenges. Transmission and distribution lines are the backbones of power systems, which whether located in rural or urban landscapes, are prone to incidents due to diverse internal and external conditions (manufacturing anomalies, thermal stress, lightning strikes, etc.). The result would be the emersion of faults and failures causing adverse effects on the quality of power supply leading to problems ranging from voltage sags and swells, insulation deterioration, or even blackouts.

Therefore, fault location and correction methods are critically important in case of any power system. This process has to be prompt and accurate so that system reliability can be improved, outage time can be reduced and restoration of system from fault can be accelerated. In this respect, the problem of fault location has received great attention with the aim of developing methods to protect power lines and cables [1]. Fault location problems in power lines have been investigated since the 1950s [2], and numerous fault location methods have been proposed. These can be classified into two main categories [3]: phasor-based (frequency domain) methods, and travelling wave-based (time domain) methods.

Although phasor-based methods are the most widely used fault location procedures as they are straightforward and

computationally-efficient approaches [4]–[6], the fault location accuracy might be affected by several factors not limited to fault impedance, power system load flow, distributed generators, and series compensation [7]. These drawbacks along with the recent improvements in data acquisition, have encouraged research on traveling wave-based (TW) techniques. TW methods rely on the analysis of fault-originating high-frequency transient signals, (i.e., travelling waves generated by the fault itself) which are relatively independent of the fault impedance [8]–[11]. By measuring the propagation delay between the first observation of the fault transient and subsequent reflections, the fault's location can be estimated knowing the velocity of propagation along the line. Single or multiple measurement points may be used. However, analyzing TW data generally requires complex signal processing techniques and the fault location accuracy is subject to several factors including time synchronization of data acquisition sensors at multiple observation points in addition to the number of sensing or observation units [12], [13].

To cope with the limitations associated with TW methods, recent studies employed time reversal (TR) processing for the analysis of TW measurements [14]. Electromagnetic TR (EMTR) as first introduced in [15] comprises two main phases. After measuring the fault transient signal from a single or multiple probes, the second phase numerically re-injects a time-reversed version of the recorded signals into a simulation-based model of the line. The fault is subsequently located by monitoring the position of the highest intensity back focusing. Various techniques have been used to differentiate the true fault location in EMTR. Their performance has been shown to depend on the kind of metric used, e.g., by monitoring

the maximum focused energy or peak amplitude [16], [17]. The authors in [18] showed that the aforementioned metrics may present non-negligible bias caused by the non-uniform distribution of high-frequency electrical energy throughout complex networks. Nevertheless, they suggested two local normalization methods in order to take into account the aforesaid counter effects [18], [19].

In classical EMTR based methods, the second phase requiring a back-injection simulation of the time-reversed measured fault signal, is accomplished for a wide range of candidate fault locations (CFLs). The CFL possessing the maximum energy or voltage depending on the metric employed, hints at the actual fault position. Indeed, it is necessary to estimate the voltage or current at each CFL, thanks to the availability of propagation models for lines and networks (e.g., numerical or theoretical). However, this can be computationally cumbersome especially when dealing with power networks whose lengths can be in the order of few Km. Although, the method proposed in [18] does not require to carry out heavy cycles of second-phase simulations for each CFL, a database containing numerically generated transfer functions for each tested network was still indispensable. On the other hand, the fact that EMTR methods are *spatially* fetching the CFL with the highest peak amplitude, creates sort of uncertainties in the ability to provide a single focusing peak, corresponding to a single CFL. This can be returned back to the intrinsic definition of TR that estimates the source's location providing the maximum coherence not only *spatially* but also *temporally*. Besides, the physical settings of EMTR methods imply the deployment of adapters at specific positions of the network so as to increase its coverage, which is not always attainable.

Accordingly, we present in this paper FasTR, a method based on the tenets of EMTR, but proposing an alternative technique to get rid of the ponderous simulation stage. For this, the first phase of FasTR method requires the implementation of at least two observation points employed at distinct positions of the network under test (NUT). Having recorded the fault-originating transients, we express analytically, but in a simplified manner, the voltage (or the current) at any position $x$ and any instant $t$ of the NUT. This is followed by constructing a cost function representing an estimate of the signal measured at any $t$ and at each $x$ of every segment of the network resulting from the back-injection, at each observation point, of the recorded time-revered signals. In other words, the cost function aims at estimating the signal corresponding to the superimposition of the different signals time-reversed and injected at each end of the network where an observation point (sensor) exists. The extremum of this cost function will eventually be *temporally* and *spatially* pointing at the fault's location. Particularly, thanks to the wide selection and advances in optimization algorithms, extracting the cost function's extremum became straightforward. It's worth noting that FasTR follows a similar analogy of applying TR to power network diagnosis than DORT method applied on communication networks [20], [21]. However, the only difference occurs at the level of the measuring phase, where instead of recording transients of an active fault generating a wave, DORT and its variants deal with passive faults that necessitate the injection of testing signals at the network extremities to enable recording the resulting fault related-reflections.

The structure of this paper is as follows. Section II recalls the basic principles of TR and revisits the definitions employed in EMTR when applied to fault location in transmission lines. The last part of this section points some fundamental limitations of EMTR, particularly the fact of providing a single focusing peak, and, therefore, a single candidate position for the fault. Section III starts by recapping electromagnetic transients originated by faults in power systems, and then establishes the basics of the simplified analytical model for the time-reversed signals' cost function. The section is ended by detailing the algorithm followed by FasTR to locate faults in NUTs. In Section IV, the applicability of FasTR is checked by simulation, where two different elevated complexity networks are considered, a single and double Y-junction networks. The results obtained are analyzed in the last part of the section. Section V reports the experimental validation of the proposed methodology using a reduced-scale model while section VI discusses the differences of wave propagation between the used reduced-scale model and real MV networks. Finally, Section VII concludes this paper by addressing the final remarks on the performance of the proposed method and proposes some perspectives.

## II. EMTR IN A NUTSHELL

### A. Time Reversal Invariance

Generally, a generic system is said to be TR invariant with respect to a physical quantity if, given a solution $g(t)$ to its underlying time-domain differential equations, the time-reversed function $g(t)$ is also a solution. However, from a practical point of view, the TR operation as defined can't be applied. Instead, for a specific time window $T$ during which $g(t)$ is recorded, $g(t)$ can be time-reversed under the form of $g(T-t)$ while ensuring the causality requirements [22]. Back-propagating $g(T-t)$ shall enable the system to retrace back its previous state, i.e. refocus on the initial source location. The system is thus referred to as *TR invariant*.

### B. EMTR applied for fault location along transmission lines

Mathematically, an equation is defined as *time reversal invariant* if it is invariant under the application of the time-reversal operator. By making reference to the TR invariance of telegraph's equations, that describe the voltage wave propagation along a multi-conductor lossless transmission line in distance and time, EMTR has been applied for fault location in power networks [15].

The EMTR fault location technique is based on two major phases: the forward propagation phase (FPP) and the backward propagation phase (BPP). In the FPP, the fault originating transient (FOT), which is a high frequency, short duration signal resulting from a sudden change affecting the network, is recorded using probes on a single or multiple observation points.

In the BPP, a simulation model of the tested network considering the same NUT parameters is then created, and a

set of CFLs is considered. In fact, based on a specific position step criterion, the CFL $x_f$ is varied along the length of the network. At each $x_f$, the recorded FOT is time-reversed and back-injected into its corresponding network numerical model. The voltage $v_f(t; x_f)$ or current $i_f(t; x_f)$ at $x_f$ is measured. Accordingly, multiple simulations depending on the number of CFLs is required. By TR theory, the back-injected signals shall focus on the source point, i.e. the CFL corresponding to the actual fault's location. The best estimate CFL $\hat{x}_f$ is identified as the one that maximizes the energy or the 2-norm, i.e.,

$$\hat{x}_f = \operatorname*{argmax}_{x_f} \|v_f(t; x_f)\|$$

with $\|v_f(t)\|$ being the fault signal energy (FSE) of $v_f(t)$ [15]. Different studies have investigated various techniques to differentiate the true fault location in the EMTR process using different norms [17], [23]. For instance, the $\infty$-norm criterion (i.e., amplitude peak criterion) introduced in [16] shows better robustness against noise compared to the 2-norm.

EMTR has proven its applicability to inhomogeneous media (for example, network composed of overhead lines and underground cables) and complex system topologies. More importantly, it has been validated through an experimental setup [15], a full-scale experiment in an un-energized overhead distribution lines [24], and on an energized medium voltage feeder [25].

### C. Limitations of the EMTR

The accuracy of the EMTR method regardless of the norm employed, is a function of the number of CFLs. Particularly, the current EMTR norms require a normalization process with respect to the maximum signal energy value for all CFLs, before locating a fault. Accordingly, such normalization is bound to have a qualitative nature as it is tied to change for each new CFL which implies a non-quantitative interpretation of the obtained results [18]. Therefore, it will be hard to decide whether to stop or not the searching criteria after each CFL.

Besides, the state-of-art of EMTR has shown that the CFL $x_f$ with the highest peak amplitude (HPA) is identified as being the potential fault position. However, the intrinsic definition of TR shows that only the HPA occurring at $t = 0$ after having injected the TR signals in the BPP, is expected to produce maximum coherence, with time and spatial focusing. Accordingly, the search criteria for locating the fault shall imperatively consider the HPA accompanied with the TR coherence at $t = 0$.

More importantly, the proper application of EMTR relies on a well-defined network topology, and an *apriori* knowledge of the fault type and impedance. Nevertheless, such information is not always available. In fact, this can put a strong limitation on the performance of the EMTR methods amid the absence of sufficient network or fault related data. Besides, it can confine the implementation of EMTR to a restricted number of fault types.

On the other hand, since EMTR based methods employ a single observation point, it necessitates the presence of
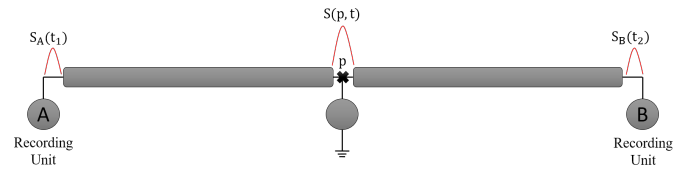


Fig. 1. A FOT generating a shock wave that propagates along a single segment transmission line and recorded at the extremities.

adapters to fix the loads on the network extremities. This was meant to ensure the occurrence of rebounds or multiple reflections at these points so that to increase the network coverage.

### III. BASIC CONCEPT OF THE FASTR TECHNIQUE

The extremities of electrical networks in power grids are usually coupled to transformers, generally behaving as capacitors with capacitances in the order of few hundreds of pF. Accordingly, they are characterized by impedances much bigger than the surge impedance of power lines. Therefore, the network is expected to act as a set of coupled resonators for FOT signals thus giving them a reverberating response. Such response has a positive effect on TR based methods as inherently an increasingly longer sequence of echoes systematically leads to a higher fraction of energy being concentrated into the peak echo.

On the basis of the aforementioned observations, we will propose FasTR method, an approach that still maintains the interpretation introduced by standard TR for the need to actually inject TR signals into the system. FasTR extends the possibilities of monitoring power networks on a larger scale by placing sensors, for continuous monitoring, on well-chosen nodes of the network. By using an accurate shared time synchronization system between sensors, transient signals can be recorded with precision and then processed on-the-fly with the FasTR algorithm. No *apriori* information of the fault type is assumed.

### A. Background

A fault event in a power network is generally associated with the generation of a step-like shock wave, triggered at the fault location, which travels along the lines of the network and gets reflected at the line extremities. For a simple point-to-point transmission line with two ends A and B as that presented in Fig. 1, a fault occurs at instant $t$ and position $p$. In the FPP, the FOT $S(p, t)$ propagates along the NUT and is recorded at extremities A and B as $S_A(t_1)$ and $S_B(t_2)$ respectively, by measurement units, e.g oscilloscopes, over a specific period $T$.

In the second BPP, the recorded signals are time-reversed as $S_A(T - t_1)$ and $S_B(T - t_2)$ and synchronously re-injected back into a simulation model of the same NUT at extremities A and B respectively. By TR theory, the signals are supposed to constructively interfere at the fault's position. To be able to locate the fault, it would be necessary to simultaneously record, at all points of the transmission line, the voltage or

current in order to detect the instant and location of the re-focusing. Despite the fact that numerous methods have been employed to solve telegraph's equations, they can be extremely heavy in terms of computation time and memory occupation especially for large power networks when a finely resolved fault localization is needed.

Accordingly, FasTR proposes a simplified manner to represent the voltage (or current) at any position on the cable network and at any instant. This is followed by searching for the extrema of this function based on a constrained optimization algorithm.

### B. FasTR algorithm

The application of FasTR to locate faults in a power network is based on the following steps:
1) the FOT is measured at predefined nodes of the NUT where sensors are placed;
2) the recorded measurements are time-reversed and numerically re-injected into a simulation model of the network;
3) a cost function $F(x,t)$ is constructed which aims at estimating the signal corresponding to the superposition of the back-propagated time-reversed signals, at each instant $t$ and position $x$ of a point in the network;
4) a searching mechanism for detecting the extremum of $F(x,t)$ is finally launched.

Each point $x$ is evaluated as the distance of the fault to each node of the NUT where an observation point exist.

To illustrate analytically $F(x,t)$, we consider the single Y-junction network of Fig. 2. The network is composed of three branches $b_i$, (i=1,2, and 3), with a supposedly occurring FOT at a random point M of segment $b_2$ and sensors placed at all extremities of the network. The transients resulting from the generated shock wave at the fault's position are recorded at each of the NUT's extremities. For each branch, the cost function $F(x,t)$ is calculated by summing up the different time-reversed back-injected signals which are also time-delayed by the propagation time of a wave between the measurement point (which is also the simulated injection point) and a point of the network with coordinate $x$. Therefore, the cost function for a segment $b_i$ is represented as follows:

$$\forall (x,t) \in \omega_b \times [0, T_{rec} + T_{max}],$$

$$F(x,t) = \sum_{e=1}^{n_r} \left[ Sr_e \left( x, t - \frac{d(x,x_e)}{v_{b_i}} \right) \right] \quad (1)$$

$\omega_b$ is the set of points of branch $b_i$ of the NUT, $T_{rec}$ and $T_{max}$ are respectively the total recording time of the signals and the time taken by a signal to travel the maximum distance present in the network. $n_r$ is the total number of extremities employing measurements devices. Notably, $n_r$ is at least two and no more than the number of ends of the network. $Sr_e$ is the time-reversed version of the signal measured at extremity $e$ with ($e \in [1, n_r]$), while $d(x,x_e)$ is the distance between any point of the network, of coordinate $x$, and an end of the NUT of coordinate $x_e$. On the other hand, $v_{b_i}$ is the velocity

of signal propagation along branch $b_i$, thus $d(x,x_e)/v_{b_i}$ is the time taken for the signal to travel the distance $d(x,x_e)$.

The literature of fault detection in power networks has long discarded the effect of cable losses on the applicability of the proposed techniques. However, since losses are inherent to transmission lines, $F(x,t)$ is modified so that to take into account the attenuation factor $\alpha_{b_i}$ of waves propagating along each branch $b_i$. The cost function hence becomes

$$F(x,t) = \sum_{e=1}^{n_r} \left[ Sr_e \left( x, t - \frac{d(x,x_e)}{v_{b_i}} \right) \times e^{\alpha_{b_i} d(x,x_e)} \right] \quad (2)$$

Besides, since power networks are mostly radial shaped, several junctions connect up segments to form the network. Accordingly, in order to be capable of testing branched networks, the cost function shall consider the energy losses of the signal during passing through a node. In the NUT of Fig. 2, when the FOT generated at M and propagating towards extremity $C_1$, passes through the junction, only a portion of its energy is transmitted towards $C_1$ and the rest is reflected back. In effect, $F(x,t)$ can be now presented as

$$F(x,t) = \sum_{e=1}^{n_r} \left[ Sr_e \left( x, t - \frac{d(x,x_e)}{v_{b_i}} \right) \times \frac{e^{\alpha_{b_i} d(x,x_e)}}{C_e^{b_i}} \right] \quad (3)$$

$C_e^{b_i}$ is the aggregated transmission coefficient between the extremity $e$ and branch $b_i$. For networks composed of several junctions, $C_e^{b_i}$ is obtained by multiplying the transmission coefficients associated with each junction crossed.

Once the cost functions of all segments composing the network are computed, the search for at least one extremum of each $F(x,t)$ is performed by means of an optimization algorithm. We adopted in our study the genetic algorithm, a dynamic random-search oriented optimization approach, that has proven efficiency in solving inverse problems [26]. Having retrieved the extrema of all segments, a single extremum is sought among them, and its corresponding coordinates $(x_f, t_f)$ are retained. The latter coordinates provide the position of the fault through $x_f$, and makes it possible to determine the instant at which the FOT has occurred via $t_f$.

More importantly, FasTR can still locate multiple faults occurring in the NUT, where instead of searching for a single extremum a plurality of extrema can be targeted. However, the search algorithm must be coupled to a detection threshold that makes it possible to discriminate the extrema corresponding to events associated with faults from those corresponding to noise-related artefacts.

It is worthy to note that the cost function evaluation presented in eq. 3 shows that segments of different parameters can be considered. However, one shall take into account each $b_i$'s surge impedance, attenuation, and velocity of wave propagation. That being said, FasTR method is applicable on non-homogeneous networks composed of several types of cables, e.g overhead lines and underground cables.

## IV. APPLICATION OF FASTR METHOD TO FAULT LOCATION

In the scope of a simulation campaign, FasTR method has been tested on a single and double Y-junction networks as shown in Figs. 2 &3 respectively. The objective was to demonstrate the capabilities of the method to converge to a fault location in the cases of complex network topologies. We considered in this work a FPP based on recording units on all the network's extremities. This shall not bring any limitation to FasTR, as the analytical model has proven the need of at least two sensors.
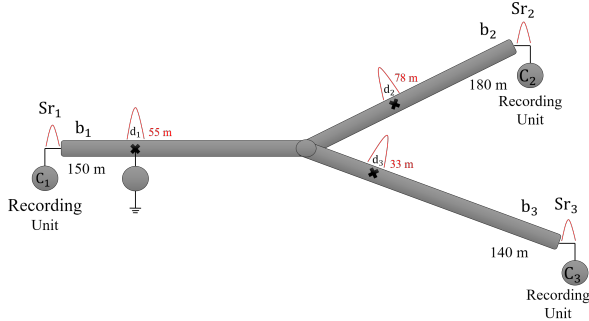


Fig. 2. Schematic of the single Y-junction network used in the first series of numerical simulations.

The first series of tests were made considering the single Y-junction NUT presented in Fig. 2. The network consists of a succession of coaxial cables with a cross-section of 95 $mm^2$, representative of cables encountered in underground medium voltage networks. The model of the junction is supposed to be perfect and the impedance at each extremity is connected to an open circuit (power transformer equivalence). The transfer function of the network is calculated through cascading the segments composing the NUT by the ABCD matrix model generated via the knowledge of the RLCG parameters of the cable. A matrix is generated for each part of the network, and the connections are mathematically materialized by a matrix product. The RLCG model used to generate the matrix of each element is dependent on frequency to integrate attenuation losses, as well as dispersion. A sensor is placed on each extremity to cover the entire topology, but none is used at the junction point.
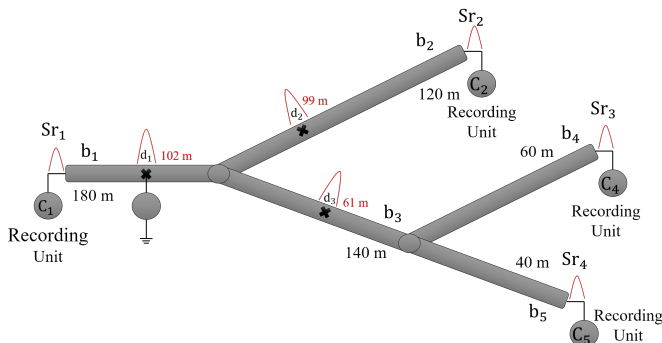


Fig. 3. Schematic of the double Y-junction network used in the second series of simulations.
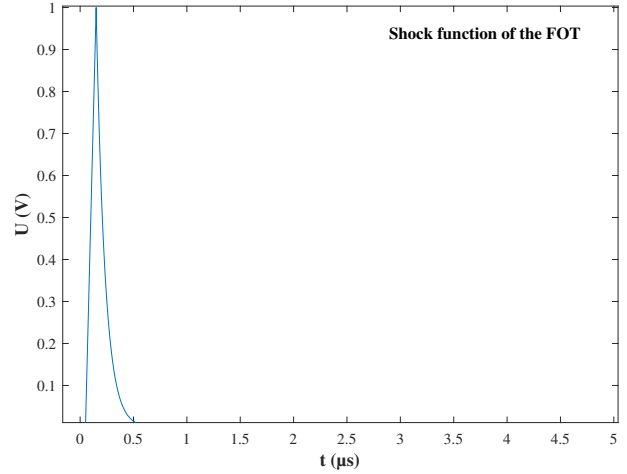


Fig. 4. Representation of the shock signal used in the simulations.

TABLE I
RESULTS OF THE APPLICATION OF FASTR METHOD ON THE SIMULATED SINGLE Y-JUNCTION NETWORK.

| Single Y-Junction NUT | | | |
|---|---|---|---|
| Fault Location | | Branch Position | |
| Actual | Estimated | Actual | Estimated |
| 55 m | 55 m | $b_1$ | $b_1$ |
| 78 m | 77 m | $b_2$ | $b_2$ |
| 33 m | 33 m | $b_3$ | $b_3$ |

The FOT is modelled by a "shock" wave, presented in Fig. 4. The first edge is a linear function of time, which lasts 0.1 µs, and the second one is an exponential relaxation with a characteristic time of 0.5 µs. This is a crude but efficient model of a sudden short-circuit followed by a capacitance relaxation due to the cable impedance. The time of generation of the defect is unknown for the sensors. However due to this lack of information, there is a need for synchronicity between the sensors to make sure that they all share the same time when collecting data. This is meant to time-stamp the instants of arrival of the FOT at each extremity. In the simulation process, this synchronicity is implicit.

### A. Single Y-junction network

A FOT is generated on three different locations along the single Y-junction NUT covering all branches as demonstrated in Fig. 2. These positions were randomly chosen on all branches so as to avoid a bias of a particular positioning, e.g. on the middle of the branch. Having recorded the transient signals on the network extremities, FasTR method as detailed in sec. III-B is applied with general information of the global topology.

The results obtained are described in table I. They show an excellent behaviour of the FasTR method for this case. The error is minimal and the faulty branch is correctly identified each time.

### B. Double Y-junction network

For the sake of testing the applicability of the proposed approach on more complex networks, FasTR is also applied

TABLE II

RESULTS OF THE APPLICATION OF FASTR METHOD ON THE SIMULATED
DOUBLE Y-JUNCTION NETWORK.

| Double Y-Junction NUT | | | |
|---|---|---|---|
| Fault Location | | Branch Position | |
| Actual | Estimated | Actual | Estimated |
| 102 m | 103 m | $b_1$ | $b_1$ |
| 99 m | 98 m | $b_2$ | $b_2$ |
| 61 m | 61 m | $b_3$ | $b_3$ |

to the double Y-junction NUT of Fig. 3. Due to a topological symmetry, the results on branches $b_4$ and $b_5$ can be extrapolated from the results of the three previous branches. Accordingly, the difference in length between branches $b_1$, $b_2$, $b_4$ and $b_5$ does not matter. The obtained results are presented in table II. Once again, the results show an eminent performance of FasTR method with an increased network complexity. The precise fault location as well as the correct branch are recognized.

### C. Analysis of the simulated cases

The results presented in the numerical validation show that FasTR method produces the expected outcome within the context of complex networks. The mathematical principle developed is coherent for the localization of the fault position with a limited knowledge of the propagation parameters. Only the topology and the celerity in each branch is known. When used, FasTR gives precise results with an error limited to the order of the meter in the tested cases. The processing time is quite similar for each case and is around 60 seconds with a common state-of-art computer. This time of calculus is directly linked to the optimization algorithm used as described previously. Here, a genetic algorithm was used and the time of calculus was a limitation set by the operator to ensure the convergence of the algorithm with a high precision. However, this time can be reduced with a compromise on the precision. In the case of an on-site use, a shorter time of calculus can be set if the order of magnitude for the error is not the priority for the troubleshooting and maintenance of the network.

## V. REDUCED SCALE EXPERIMENTAL VALIDATION

In this section, the experimental validation of the proposed method is presented by making reference to a reduced-scale coaxial cable system. Such a system has been realized by using standard RG58 coaxial cables where real faults were hardware-emulated. A single Y-junction network was assembled with BNC connectors while a BNC T-port formed the junction. Fig. 5 shows the schematic of the assembled network consisting of three lines of lengths 30 m, 29 m and 12 m respectively. We choose two positions for the fault on the branch terminated with sensor $C_3$, at respectively 5 m and 10 m from the junction.

To generate the fault, an Arbitrary Waveform Generator (AWG) was connected at the position of the fault locations through a BNC T-port each at a once. The FOT is a slow rate shock signal adapted to the short lengths of the branches considered. The rise time and fall time for the transient were
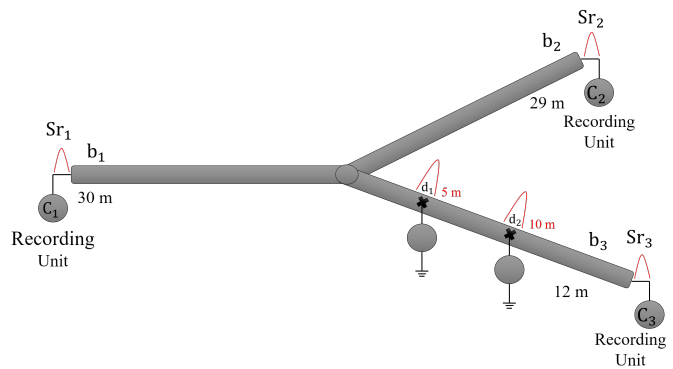


Fig. 5. Topology adopted for the reduced-scale experimental setup.
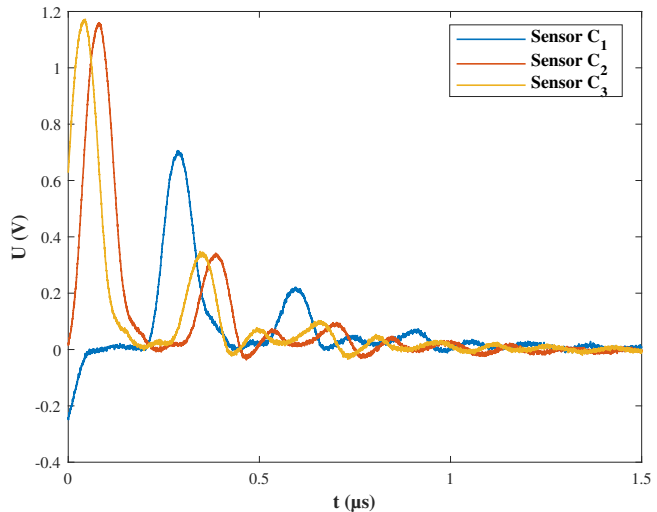


Fig. 6. The direct-time experimentally measured waveforms for a fault location at 5 m from the junction of the NUT of Fig. 5.

set to 50 ns while the up time was set to the minimum authorized by the device: 80 ns. Recording the transients at the NUT's extremities was performed with a LeCroy Digital Oscilloscope WaveRunner 9000 operating at a sampling rate of 2GS/s. The three branches of the network were connected to a measurement channel with a high impedance coupling and the injection signal was also measured to allow the synchronicity in the measurements, even though it was not involved in the FasTR calculus. Fig. 6 shows the signals measured in the FPP on the three sensors for the FOT generated at position $d_1$.

In the BPP, FasTR approach was applied where the measured signals were time-reversed and numerically re-injected at the three extremities of a simulation model of tested network. This is followed by constructing the cost function $F(x,t)$ for each of the two faults positions whose extrema returned 4.37 m and 9.7 m on branch $b_3$ respectively. The post-processing calculus lasted around 60 s for each case. Accordingly, it is possible to infer the remarkable performance of the proposed fault-location method for the case of a realistic network.

## VI. PERFORMANCE DISCUSSION ON THE REDUCED SCALE VALIDATION

The previous section has presented a reduced-scale model as a basis for demonstrating the FasTR method's applicability on

real-networks. FasTR has accordingly proven to reliably detect and locate faults with high precision. However, the proposed experimental model is not representative of a real MV network for there are many differences in wave propagation between the two cases.

First of all, MV networks are mainly composed of three-phases power lines whereas our demonstration network was a single-phase one. Subsequently, the presence of multiple phases generates inter-phase coupling, which in-turn modifies the propagation parameters and adds crosstalk between channels. In particular, the connection configuration (phase to phase, or phase to ground) does not lead to the same results, depending on the load of the network, the quality of grounding, etc. [27]. Besides, MV networks are often a mixed configuration of transitions between underground cables and overhead lines. These transitions add a perturbation factor in the overall link budget and each part of the network has its own propagation model, whereas the RG58 coaxial cables possess a unique model. The authors of [28] and [29] present propagation models for underground cables and overhead lines respectively.

Finally, we assumed in this paper an open-circuited behaviour of the MV/LV transformers. Although, it is the case adopted in the majority of work dealing with fault detection in power networks, the reality is more complicated. In fact, the behaviour of power transformers is a function of frequency [30]. This could be taken into account by introducing an equivalent circuit at the end of each branch composing the tested network to better represent the effect of MV components.

It is expected, knowing all these differences, that the propagated signal in our case is idealized in comparison to MV on-line transients. A higher attenuation of the signal may lead to a diminution of the detection capacity of the system but will not invalidate the principle of the method. A distortion of the signal and the addition of crosstalk may be more problematic, as it can make it more difficult to compensate in the calculus phase of the proposed method. This implies a work on reinforcing the propagation models in the calculus method or the addition of special components in the measuring device that reduce all these unwanted effects. Further study will have to take into account a more representative case to better ascertain the benefit of such a method.

## VII. Conclusion

This article presented the problematic of fault location in power networks. It firstly described the general approach using time reversal, then presented the EMTR method, based on TR Invariance. Despite the fact that this type of method has proven to allow a high precision localization of faults with a limited need for costly resources, it possessed some limitations. Particularly, these included the cumbersome post-processing of the time-reversed recorded signals in addition to the need of *apriori* information about the network, and fault's nature.

To address these limitations, and to extend the complexity of networks that can be monitored, we proposed a new method, called FasTR. This method shares the TR mathematical principles but with a clever use of topology knowledge and mathematical optimization algorithms, it circumvents the time- and resource-consuming steps of complete calculus of TR response. It allows for an on-the-fly treatment and a precise fault location in complex networks with just a basic knowledge of topology.

The efficiency of the proposed method has been demonstrated firstly with a simulation campaign on two types of networks with an increasing complexity. Several fault positions were tested on each branch of each network, and FasTR was able to precisely localize the fault (position and branch) within a minute of calculus. Errors were in the order of the meter. FasTR method has also been validated with success by means of a reduced scale experiment with laboratory equipment and real coaxial cables.

Theses results prove the relevance of the FasTR approach to fault location in complex networks. It opens the way for an on-site monitoring tool with high precision and quick response time, with a limited need for topology and field knowledge. The next step is to test it on a medium voltage network in operation. Besides, investigating multiple faults within the same network and addressing inhomogeneous complex networks with a limited number of sensors is being worked.

## References

[1] C. Furse, M. Kafal, R. Razzaghi and Y. J. Shin, "Fault Diagnosis for Electrical Systems and Power Networks: A Review," in *IEEE Sensors Journal*, April 2020, DOI: 10.1109/JSEN.2020.2987321.

[2] T. W. Stringfield, D. J. Marihart, and R. F. Stevens, "Fault location methods for overhead lines," in *Trans. Amer. Inst. Electr. Eng. III, Power App. Syst*, vol. 76, no. 3, pp. 518–529, 1957.

[3] "IEEE Guide for Determining Fault Location on AC Transmission and Distribution Lines." 2005, DOI: 10.1109/IEEESTD.2005.96207.

[4] M. S. Sachdev and R. Agarwal, "A technique for estimating transmission line fault locations from digital impedance relay measurements," in *IEEE Trans. Power Del.*, vol. 3, no. 1, pp. 121–129, Jan. 1988.

[5] K. Srinivasan and A. St.-Jacques, "A new fault location algorithm for radial transmission lines with loads," in *IEEE Trans. Power Del.*, vol. 4, no. 3, pp. 1676–1682,Jul. 1989.

[6] A. A. Girgis, D. G. Hart, and W. L. Peterson, "A new fault location technique for two- and three-terminal lines," in *IEEE Trans. Power Del.*, vol. 7, no. 1, pp. 98–107, Jan. 1992.

[7] F. V. Lopes, K. M. Silva, F. B. Costa, W. L. A. Neves, and D. Fernandes Jr, "Real-Time Traveling Wave-Based Fault Location Using Two-Terminal Unsynchronized Data," in *IEEE Trans. Power Del.*, vol. 30, no. 3, pp. 1067–1076, 2014.

[8] P. F. Gale, P. A. Crossley, X. Bingyin, G. Yaozhong, B. J. Cory, and J. R. G. Barker, "Fault location based on travelling waves," in *in Proc. 5th Int. Conf. Develop. Power Syst. Protection*, Mar. 1993, pp. 54–59.

[9] G. B. Ancell and N. C. Pahalawaththa, "Maximum likelihood estimation of fault location on transmission lines using travelling waves," in *IEEE Trans. Power Del.*, vol. 9, no. 2, pp. 680–689, Apr. 1994.

[10] A. O. Ibe and B. J. Cory, "A travellingwave-based fault locator for two- and three-terminal networks," in *IEEE Trans. Power Del.*, vol. 1, no. 2, pp. 283–288, Apr. 1986.

[11] Z. Q. Bo, G. Weller, and M. A. Redfern, "Accurate fault location technique for distribution system using fault-generated high-frequency transient voltage signals," in *IEE Proceedings-Generation, Transmission and Distribution*, vol. 146, no. 1, pp. 73–79, Jan. 1999.

[12] M. M. Saha, J. J. Izykowski, and E. Rosolowski, "Fault Location on Power Networks," in *Springer Science & Business Media*, vol. 25, 2009.

[13] A. Borghetti, M. Bosetti, M. Di Silvestro, C. A. Nucci, and M. Paolone, "Continuous-wavelet transform for Fault Location in Distribution Power Networks: Definition of Mother Wavelets Inferred From Fault Originated Transients," in *IEEE Transactions on Power Systems*, vol. 23, no. 2, pp. 380–388, 2008.

[14] M. Kafal, R. Razzaghi, A. Cozza, F. Auzanneau, and W. Ben Hassen, " A review on the application of the time reversal theory to wire network and power system diagnosis," in *IEEE International Instrumentation and Measurement Technology Conference (I2MTC)*, May 2019.

[15] R. Razzaghi, G. Lugrin, H. Manesh, C. Romero, M. Paolone, and F. Rachidi, "An efficient method based on the electromagnetic time reversal to locate faults in power networks," in *IEEE Trans. Power Del.*, vol. 28, no. 3, pp. 1663–1673, Jul. 2013.

[16] S. Y. He et al., "Norm Criteria in the Electromagnetic Time Reversal Technique for Fault Location in Transmission Lines," in *IEEE Transactions on Electromagnetic Compatibility*, vol. 60, no. 5, pp. 1240–1248, Oct. 2018.

[17] Z. Wang, R. Razzaghi, M. Paolone, and F. Rachidi, "Electromagnetic time reversal applied to fault location: On the properties of back-injected signals," in *in 20th Power Systems Computation Conference*, PSCC 2018.

[18] S. Y. He, A. Cozza, and Y. Xie, "Electromagnetic Time Reversal as a Correlation Estimator: Improved Metrics and Design Criteria for Fault Location in Power Grids," in *IEEE Transactions on Electromagnetic Compatibility*, pp. 1–14, Jun. 2019.

[19] S. Y. He, A. Cozza, and Y. Xie, "On the Spatial Resolution of Fault Location Techniques Based on Full Fault Transients," in *IEEE Trans. Power Del.*, October 2019.

[20] L. Abboud, A. Cozza, and L. Pichon, "A noniterative method for locating soft faults in complex wire networks," in *IEEE Transactions on Vehicular Technology*, vol. 62, no. 3, pp. 1010–1019, 2013.

[21] M. Kafal, A. Cozza, and L. Pichon, "Locating multiple soft faults in wire networks using an alternative DORT implementation," in *EEE Transactions on Instrumentation and Measurement*, vol. 65, no. 2, pp. 399–406, 2015.

[22] F. Rachidi, M. Rubinstein, and M. Paolone, *Electromagnetic Time Reversal: Application to EMC and Power Systems*. John Wiley & Sons, 2017.

[23] R. Razzaghi, M. Paolone, F. Rachidi, J. Descloux, B. Raison, and N. Retiére, "Fault location in multi-terminal HVdc networks based on electromagnetic time reversal with limited time reversal window," in *in Proc. Power Syst. Comput. Conf.*, pp. 1–7,Aug. 2014.

[24] Z. Wang et al., "A Full-Scale Experimental Validation of Electromagnetic Time Reversal Applied to Locate Disturbances in Overhead Power Distribution Lines," in *IEEE Transactions on EMC*, vol. 60, no. 5, pp. 1562–1570, 2018.

[25] Z. Wang, R. Razzaghi, M. Paolone, and F. Rachidi, "Time reversal applied to fault location in power networks: Pilot test results and analyses," International Journal of Electrical Power and Energy Systems," in *International Journal of Electrical Power and Energy Systems*, vol.114, Jan. 2020.

[26] Z. Michalewicz, *Genetic algorithms+ data structures= evolution programs*. Springer Science & Business Media, 2013.

[27] T. A. Papadopoulos, B. D. Batalas, A. Radis, and G. K. Papagiannis, "Medium voltage network PLC modeling and signal propagation analysis," in *IEEE International Symposium on Power Line Communications and Its Applications*, pp. 284–289, March 2007.

[28] P. A. A. F. Wouters, P. C. J. M. Van Der Wielen, J. Veen, P. Wagenaars and E. F. Steennis, "Effect of cable load impedance on coupling schemes for MV power line communication," in *IEEE Transactions on Power Delivery*, vol. 20, no. 2, pp. 638–645, April 2005.

[29] D. W. Chun et al., "Impedance analysis of overhead medium voltage power lines for broadband PLC," in *IEEE International Symposium on Electromagnetic Compatibility*, pp. 196–198, 2006.

[30] C. J. Kikkert, "Power transformer modelling and MV PLC coupling networks," in *IEEE PES Innovative Smart Grid Technologies*, pp. 1–6, 2011.